

A Low-Cost Optical Sensing Device based on Paired Emitter-Detector LEDs

King-Tong Lau¹, Susan Baldwin¹, Martina O'Toole¹, Roderick Shepherd¹, William J Yerazunis², Shinichi Izuo³, Satoshi Ueyama³ and Dermot Diamond^{1*}

¹Adaptive Sensors Group, National Centre for Sensor Research, School of Chemical Science, Dublin City University, Dublin 9, Ireland.

² Mitsubishi Electric Research Laboratories, 201 Broadway, Cambridge, MA 02139, USA.

³ Advanced R&D Center, Mitsubishi Electric Corporation, 8-1-1 Tsukaguchi-honmachi, Amagasaki, Hyogo 661-8661, Japan

corresponding authors: kim.lau@dcu.ie

dermot.diamond@dcu.ie

Abstract

A low power, high sensitivity, very low cost light emitting diode (LED) based device for intensity based light measurements is described. In this approach, a reverse-biased LED functioning as a photodiode, is coupled with a second LED configured in conventional emission mode. A simple timer circuit measures how long (in μs) it takes for the photocurrent generated on the detector LED to discharge its capacitance from logic 1 (+5 V) to logic 0 (+1.7 V). The entire instrument provides an inherently digital output of light intensity measurements for a few cents. This light intensity dependent discharge process has been applied to measuring concentrations of coloured solutions and a mathematical model developed based on the Beer-Lambert Law.

Key words

Light Emitting Diode, photodiode, colorimetry, optical sensor, sensor networks.

Introduction

The vast majority of analytical measurements are currently made under specialist laboratory conditions using bench-top instruments that are designed to deliver high precision and accuracy for multiple components in samples that often have extremely complex matrices. This particularly so in important application sectors such as clinical assays, genomic/proteomic research, the pharma industry and environmental monitoring. However, it is becoming clear that developments in and availability of wireless communications (e.g. GSM, 3G, 802.11, Bluetooth, ZigBee, RFID etc.) and portable computing provide an infrastructure for the functional deployment of wireless sensor networks. While research in this area is overwhelmingly dominated by demonstrator projects employing physical

transducers, it is logical to predict that chemical sensors and biosensors will be introduced when inexpensive, reliable devices are available [1-5].

For example, sensor networks targeting important analytes may be deployed to cover a strategically important area, from where the autonomously collected data may be harvested by remote servers that seek out specific events such as threshold crossing, and trawl for patterns in larger scale information sets that may herald the initiation of an environmental pollution event, or the release of hazardous agent [6].

However, the widespread deployment of chemical sensors and biosensors can only be successfully achieved if devices with appropriate operating characteristics are available at very low cost. For example, sensor networks involving many devices will require that each sensor-node (i.e. sensor + signal acquisition electronics + wireless communication) costs a few cents or less and can operate reliably for up to years at a time while simultaneously consuming very low (virtually no) power. This concept poses significant challenges for chemical sensor/biosensor research, as no such devices are currently available, and sensor network research is therefore dominated by physical measurements such as light density and temperature. This situation has prompted us to explore various strategies for making long-term field measurements using stable reagents in a lab-on-a-chip instrument configuration [7], and simultaneously developing very low-cost device platforms for making analytical measurements [8].

Light emitting diodes (LEDs) are robust, low cost, low power, very efficient in terms of energy conversion, small size and they cover an increasingly broad spectral range from uv to near infrared. These properties are ideal for the development of optical devices and consequently LEDs have been widely used in consumer electronic devices, and in more specialist applications such the illumination source for fibre optic sensors [9-16] and reflectometers [17]. The concept of using LEDs as light detectors has already been explored by Mims et. al. These workers used a simple circuit that contained an operational amplifier to measure the photocurrent obtained by a reverse biased LED, and have used this LED-sensor for detecting sunlight intensity [18,19].

As LED-photodiodes are considerably less sensitive than commercial photodiodes (we typically find the photocurrent to be around 10-100 times smaller), direct measurement of the photocurrent is difficult without amplification, and requires an expensive picoammeter. However, our previous work [8] has shown that very accurate and precise measurement of the photocurrent is possible using a simple threshold detector and timer circuit. Basically, the sensing LED is reverse biased to +5 V (logic 1) and on switching to measurement mode, this charge is sustained by the inherent capacitance of the diode (typically picofarads). The

time taken for the photocurrent from the LED-sensor to discharge this voltage to logic 0 (+1.7 V) is measured, and is obviously related to the incident light intensity. This extremely low cost approach provides inherently digital measurement of light intensity without amplification, while simultaneously providing excellent signal to noise characteristics, due to the signal integration over the measurement. In this configuration, the sensitivity of the LED-photodiode is improved and become more attractive than a conventional (and more expensive) photodiode, which discharges the capacitor much more quickly, making time-based discrimination more difficult and expensive.

Theoretical model

A mathematical model has been developed to relate this sensing strategy to conventional analytical measurements based on the Beer-Lambert Law. Figure 1 is the LED equivalent circuit. The light-sensing LED is reverse biased to 5 V and is discharged by the photocurrent i_{light} generated by the incoming light.

Another discharging process also occurs naturally in parallel in which the circuit discharges itself in complete darkness via a small (dark) current i_{dis} , which is normally insignificant compared to i_{light} . Typically, under strong illumination, we have found the discharge time to be in the region of microseconds, whereas in complete darkness, it discharges in ca. 300 milliseconds.

In general, the total discharge time t for the LED equivalent circuit can be described as

$$t = \frac{Q}{i_{dis} + i_{light}} \quad (1)$$

where Q is accumulated charge (a constant)

When $i_{light} \gg i_{dis}$

$$t = \frac{Q}{i_{light}} \quad (2)$$

i.e; the time taken to discharge the capacitor is inversely proportional to the intensity of the incident light, as the quantity of electric charge (Q) is a constant.

When light passes through a coloured sample solution, the emitted light intensity (I) is reduced relative to the incident light intensity (I_o) due to absorbance of the light energy by the analyte at certain wavelengths. The sample absorbance (A) is related to these intensities and the sample concentration by the Lambert-Beer Law;

$$A = \log\left(\frac{I_o}{I}\right) = \epsilon Cl \quad (3)$$

where;

l = optical path length through the solution

ϵ = molar extinction coefficient (mol/l/cm) at a particular wavelength

C = concentration of the absorbing species

Substituting (2) into (3) we get;

$$A = \log\left(\frac{I_o}{I}\right) = \log\left(\frac{t}{t_o}\right) = \epsilon Cl \quad (4)$$

where t_o is the time to discharge to a preset voltage in the absence of the coloured species in solution (a constant), therefore we can say;

$$\log(t) = \epsilon Cl + \log(t_o) \quad (5)$$

Equation 5 predicts that if the Lambert-Beer law holds, and the dark current from the capacitor is negligible compared to the photo-discharge current, then the concentration of the absorbing analyte is proportional to the log of the discharge time, with the intercept being $\log(t_o)$.

Experimental

Chemicals and materials

Light emitting diodes and photodiodes used in this study were commercially available products from various manufacturers (Kingbright, LED-Tech, Agilent, Nitia-Kagak, Toshiba and Siemens).

Bromocresol green, 1,10-phenanthroline and ferrous ammonium sulphate hexahydrate were purchased from Sigma-Aldrich, Dublin Ireland. All reagents used were of analytical grade.

Optical cell construction

A simple measuring system was constructed in house (Figure 2) by firstly milling a cavity (1.3 cm length x 0.4 cm width x 2 cm height) in two separate identical pieces of black nylon (width 2 cm, height 2.8 cm, length 3.2 cm). The two sections were then joined together using black silicon glue to form a sample well (1.3 cm length x 0.4 cm width x 1.5cm height), which could hold 1 mL of solution. Two small compartment holes ($d = 5$ mm) were fabricated on opposite sides of the cell and the LEDs were secured in facing each other in perfect alignment. PMMA transparent slides (width 1.5 cm, height 2.5 cm) were fixed in front of the LEDs to seal and act as windows for the LEDs using Araldite glue (RS components, Ireland). The cell was then covered by a black nylon lid (width 2 cm x length 3.2 cm) to exclude ambient light.

Results and Discussion

Discharge of LED

The capacitance of Light emitting diodes is typically in the region of picoFarads. Hence the discharge time for such devices will be small ranging from μs under bright light to ms in low light conditions. Figure 3 is a typical discharge profile for an LED with λ_{max} of emission at 610 nm obtained from a Fluke ScopMeter[®] (Fluke Corporation, WA, USA). The LED was charged up and held at 5 V for 500 μs before being discharged under fluorescent lighting. In this case, the discharge time is ca. 132 μs .

The timer circuit we have developed to measure this discharge time offers 16 bit resolution and a sampling rate of ca. 7 data points per second. Generally, we use a sampling time of 10 second and store the average value obtained.

Validation of LED light sensor

Experiments were also carried out to verify the response characteristics of the LED light sensors. Figure 4 (inset) shows the linear relationship between increasing load (current limiting) resistance on an LED emitter ($\lambda_{\text{max}} = 620 \text{ nm}$) and the resulting light intensity observed by a light dependent resistor (LDR). This demonstrates that the LDR response (R) is increased linearly with the current limiting resistance. The response of the LDR to varying light intensity is well established such that light Intensity (I_{light}) is inversely proportional to the observed resistance (R). Therefore it can be deduced that increasing the load resistance reduces LED output intensity and that the output light intensity from an LED is inversely proportional to the current limiting resistance i.e. ($I_{\text{light}} \propto 1/R$). This experiment was repeated by substituting the LDR with an LED light sensor ($\lambda_{\text{max}} = 620 \text{ nm}$). The results (Figure 4) show that the discharge time t increases linearly with current limiting resistance, which may be expressed as the reciprocal of light intensity, and is therefore in agreement with equation 2 (i.e. $t \propto 1/I_{\text{light}}$) up to a limiting value where the incident light intensity is too low to be distinguished.

Comparison of various LEDs as light detectors

Using a constant emitter LED (emission $\lambda_{\text{max}} = 660 \text{ nm}$) as an energy source, and series of neutral density filters to vary light output intensity (relative intensities of 1, 2.8 and 8.3), the effect of LED λ_{max} on the sensitivity of LED light sensors was investigated. The results (Figure 5) show that the LEDs have a linear response to the inverse of incident light intensity, as predicted by equation 2. Discharge rate is fastest for the 660 nm LED sensor, and the discharge time increases with decreasing λ_{max} . The 567, 470 and 430 nm LEDs did not produce a photocurrent large enough to be detected by the timer circuit. In LEDs, the photon energy distribution is centred on the λ_{max} , with a relatively small spread, defined by the corresponding distribution of energy levels (bandgap) in the semiconductor. In light-sensing mode, the same energy level distributions are involved, and generation of charge carriers can only happen if the incoming photons have enough energy to generate electron transitions across these energy levels. In the case of the 567, 470 and 430 nm LEDs, the bandgap is too great for the incoming photons centred on 660 nm to cause transitions. As the λ_{max} of the LED sensor increases towards 660 nm, the bandgap becomes correspondingly smaller, the population of photons capable of causing transitions increases, resulting in smaller discharge times from the measurement circuit.

Comparison to photodiodes

Photodiodes (PDs) are known to be much better light detector than LEDs because they are configured to optimise light detection rather than to emit light. Therefore a PD would be much more sensitive than an LED when measuring the photocurrent output directly upon light irradiation. However, LED light detector based on measuring charge decay time improves the sensitivity significantly by noise reduction inherent to this technique and by using data averaging. The response characteristics of PDs to varying light intensity were compared to those of LEDs. It has to be stressed that it is *the sensitivity to a change in light intensity* that is important to an intensity-based optical detector. On the other hand, the detector has to offer sufficient sensitivity to low light intensity to detect high concentration of light absorbing species.

Five commercially available photodiodes were used in the circuitry replacing LEDs for light measurement. Figure 6 shows that similar linear plots to those shown in Figure 5 were generated by PDs, which suggests that LEDs and PDs are interchangeable in this mode of light measurement. However, It can be seen by comparing Figure 5 and Figure 6 that photodiodes are (approximately 10 times) more efficient in producing photocurrent and therefore, discharged at a much faster rate than their LED counterparts. However, the lower photocurrent producing efficiency by LEDs turns out to be an advantage in this particular mode of operation. It can be clearly seen that the slopes of response to light intensity by LED detectors are approximately an order of magnitude higher than those obtained by PDs (The range of slopes observed for PDs are ca. $0.3 - 3 \times 10^2 \mu\text{s/unit}$ whereas for LEDs the observed values are ca. $0.3 - 5 \times 10^3 \mu\text{s/unit}$). The inset in Figure 6 compares the responses from an LED detector and a PD in situation when the light source bandgap overlaps with that of the detectors. In this case the slope obtained for LED detector was $274.5 \mu\text{s/unit}$, which was 8 times higher than that obtained with a PD ($34.9 \mu\text{s/unit}$). These data has shown that this technique has reversed the order of sensitivity observed by the conventional method that measures directly photocurrent and that LED detectors operated in this proposed technique are superior to PDs.

Colour Measurement with paired LED sensor system

Using the optical cell described in Figure 2, the effectiveness of a paired LED emitter-sensor for photometric measurements was investigated. Various concentrations of bromocresol green solutions made up in pH7 buffer were placed into the optical cell and the transmitted light intensity measured by the LED detector ($\lambda_{\text{emitter}} = \lambda_{\text{detector}} = 610 \text{ nm}$) which overlaps strongly with the absorbance spectrum of the dye. The log of the discharge times ($\log t$) obtained were plotted against dye concentration (c) (Equation 5), and a straight line

with R^2 value of 0.998 was obtained (Figure 7a). The lowest dye concentration detected was 0.1 μM as shown in Figure 7b. This real time response trace showed that the discharge time (response obtained) for the baseline was $12884 \pm 10.9 \mu\text{s}$ for $n=20$ data points; whereas the response obtained for 0.1 μM BCG was, for $n=20$, $13004.8 \pm 17.5 \mu\text{s}$, which just exceeded the threshold value of 12985 μs calculated from [baseline + 3 standard deviation]. These results demonstrate that, even without significant optimisation, the system can be used for analytical measurements with excellent precision and sensitivity (to sub-micromolar levels), and that the mathematical model described by equation 5 is obeyed. Furthermore, the sensor response is very rapid, reaching equilibrium in around 4 s to an addition of 1 μM BCG (Figure 7b).

We also used the same LED combination to determine Iron II in water using 1,10-phenanthroline as the complexing agent to form a red coloured complex ($\lambda_{\text{max}} = 610 \text{ nm}$). Once again, a very precise linear relationship between the log of the discharge time (t) and concentration of the absorbing species is obtained (Figure 8), with a linear range up to around 300 μM and a detection limit of ca. 5 μM .

Conclusion

These results demonstrate that this very low-cost emitter-detector LED arrangement and timer circuit can be used to make very sensitive analytical measurements. Excellent signal-to-noise characteristics are obtained because of the signal integration during measurements. The circuit provides a digital output, and the sensitivity can be tuned using a variable load resistor on the emitter LED to vary incident light intensity. The entire system can be integrated into a small, inexpensive, low-power package for analytical applications. The diodes can be arranged to make transmission measurements (as in this paper) or for reflectance measurements. This latter arrangement is very useful for monitoring changes in the colour of chromo-responsive dyes immobilised on surfaces (e.g. diagnostic tests, smart packaging) or to monitor colour in flow or microfluidic systems. In addition, one or both diodes can be coated with coloured reagents to provide an inherent chemical sensing function, and an array of devices with differing λ_{max} used cooperatively to generate complementary information for simultaneous multicomponent assays.

Furthermore, LEDs can be used to send/receive data over distances of up to 1 metre [19], and the LEDs themselves can indicate status visually over relatively long distances using digital cameras as monitors. Hence the platform also has the potential to store and transmit data on demand to an external device. Coupled with a longer range (but low-cost and low-power) wireless communication capability, this device, in its various configurations, has the

capability of becoming a fundamental building block (or chemical sensing node) for wireless sensor networks.

Acknowledgements

The Authors wish to thank Science Foundation Ireland SFI for grant support under the Adaptive Information Cluster Award (SFI 03/IN3/1361).

References

1. Kochhal M, Schwiebert L, Gupta S., J. Science Engineering and Computing, 20 (2004) 449-475.
2. Mehta V., El Zarki M., Wireless Networks, 10 (2004) 401-412.
3. Mini R.A.F., Loureiro A.A.F., Nath B., Computer Communications, 27 (2004) 935-945.
4. Yang X.P., Ong K.G., Dreschel W.R., Zeng K.F., Mungle C.S., Grimes C.A., Sensors 2 (2002) 455-472.
5. Grimes C.A., Ong K.G., Varghese O.K., Yang X.P., Mor G., Paulose M., Dickey E.C., Ruan C.M., Pishko M.V., Kendig J.W., Mason A.J., Sensors 3 (2003) 69-82.
6. Diamond D., Analytical Chemistry (2004), in press.
7. Bowden A., Diamond D., Sens. Actuators B 90 (2003) 170-174.
8. King Tong Lau, Susan Baldwin, Roderick L. Shepherd, Paul H. Dietz, William. S. Yezunis and Dermot Diamond, Talanta, 63 (2004) 167-173.
9. Mizaikoff B., Water Science and Technology, 47 (2003) 35-42.
10. Primak I.U., Sotskaya L.I., Optical and Quantum Electronics, 35 (2003) 275-287.
11. Okura I., J Porp and Phthalocyanine, 6 (2002) 268-270.
12. Canada T.A., Allain L.R., Beach D.B., Xue Z.L., Anal. Chem., 74 (2002) 2535-2540.
13. Lechuga L.M., Quimica Analitica, 19: Suppl. 1 (2000) 61-67.
14. Ghosh A.K., Bedi N.S., Paul P., Optical Engineering, 39 (2000) 1405-1412.
15. Freiner D., Kunz R.E., Citterio D., Spichiger U.E., Gale M.T., Sens. Actuators. B, 29 (1995) 277-285.
16. Matias F.A.A., Vila M.M.D.C., Tubino M., Sens. Actuators B, 88 (2003) 60.
17. Mims, Forrest M., Applied Optics, 31, No. 33. (1992) 6965-6967.

18. Mims, Forrest M., *Scientific American*, 263 (2): (1990) 106-109.
19. Paul Dietz, William Yerazunis, Darren Leigh, International conference on ubiquitous computing, Ubicomp, october, 2003. Full text can be access at <http://www.merl.com/publications/TR2003-035/>.

List of Figures

Figure 1. A schematic of LED equivalent circuit.

Figure 2. A Schematic of the detector cell used for chemical sensing.

Figure 3. Typical discharge curve for an LED charged up to 5 V and then discharged to a threshold of 1.7 V under artificial lighting (fluorescent tube).

Figure 4. Decay time of detector LED versus the current limiting resistance used to control intensity of the emitter. The emitter-detector LEDs were 1 cm apart. Inset is a linear plot obtained by increasing current limiting resistance applied to an LED emitter circuitry which results in a change in light intensity measured with a light dependent resistor.

Figure 5. Detection characteristics of LEDs with varying λ_{\max} configured as light sensors. The source used was an LED with emission λ_{\max} at 660 nm.

Figure 6. Detection characteristics of various commercial PD light sensors using decay time light measuring regime. The source used was an LED with emission λ_{\max} at 660nm. Inset is the plots from a PD and an LED when the 660nm LED light source band gap matches the detectors. The LED detector shows better sensitivity than the PD.

Figure 7. (a) A plot of LED sensor discharge time (Log t) versus BCG dye concentration (n=3 and $\text{rsd} < 0.1\%$). (b) The real time response of the system to additions of BCG at low concentrations

Figure 8. Calibration plot for 1,10-phenanthroline-Iron II complex detection using paired LED sensor system (n=3).

Figure 1

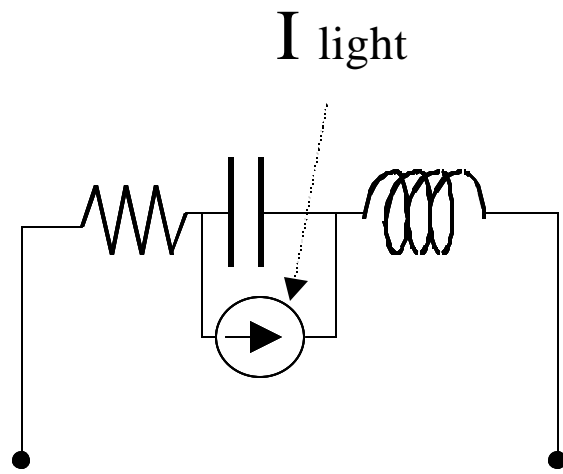


Figure 2

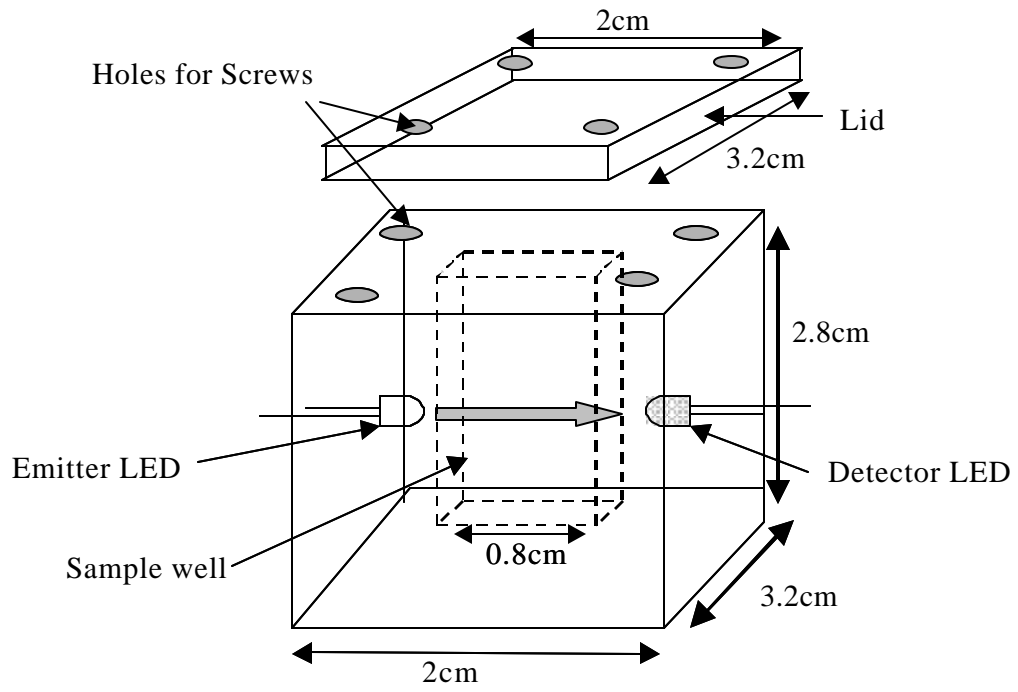


Figure 3

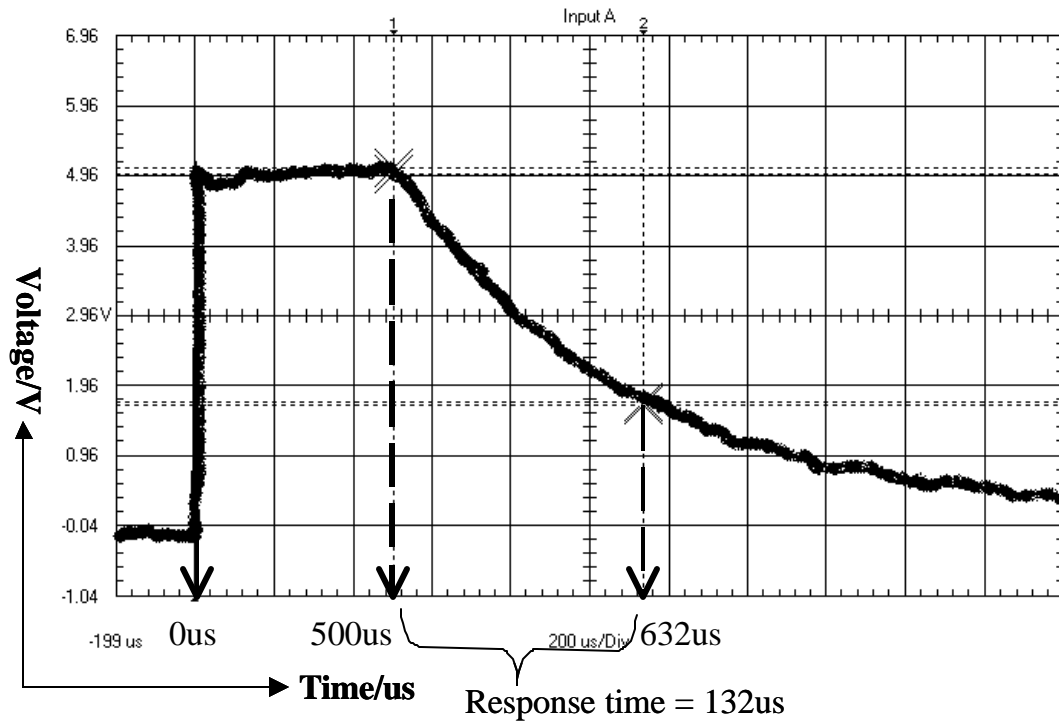


Figure 4

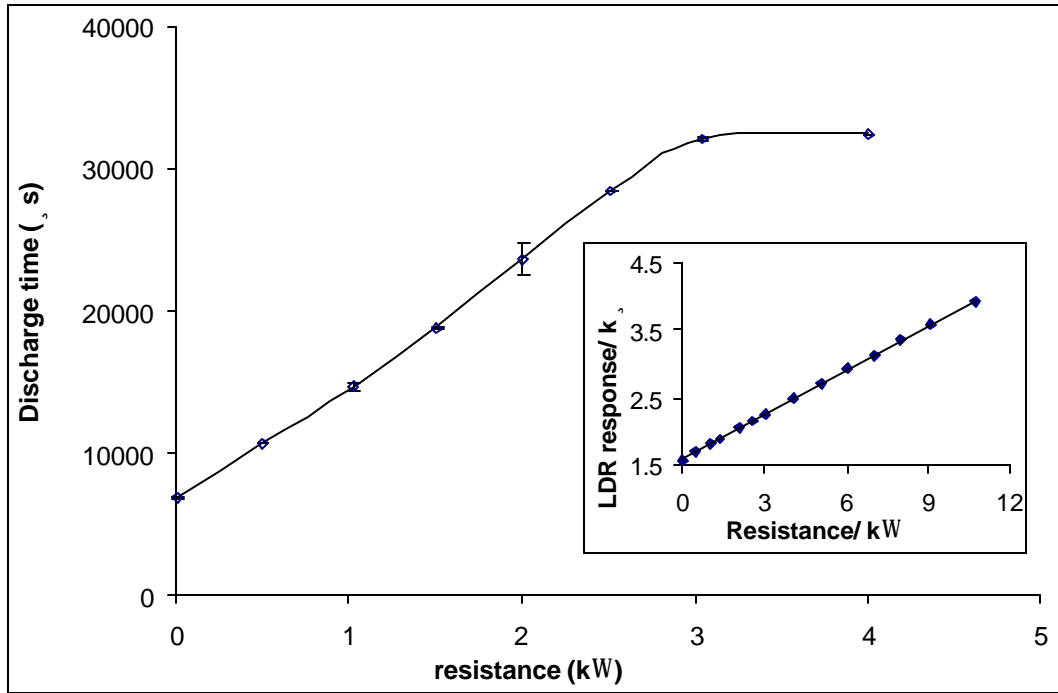


Figure 5

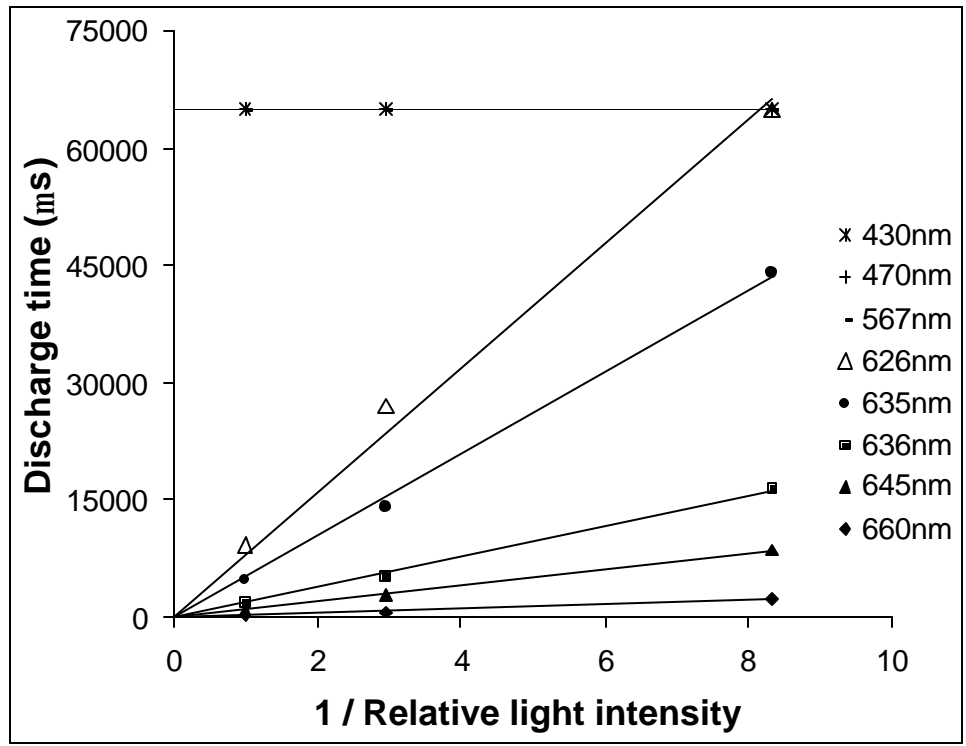


Figure 6

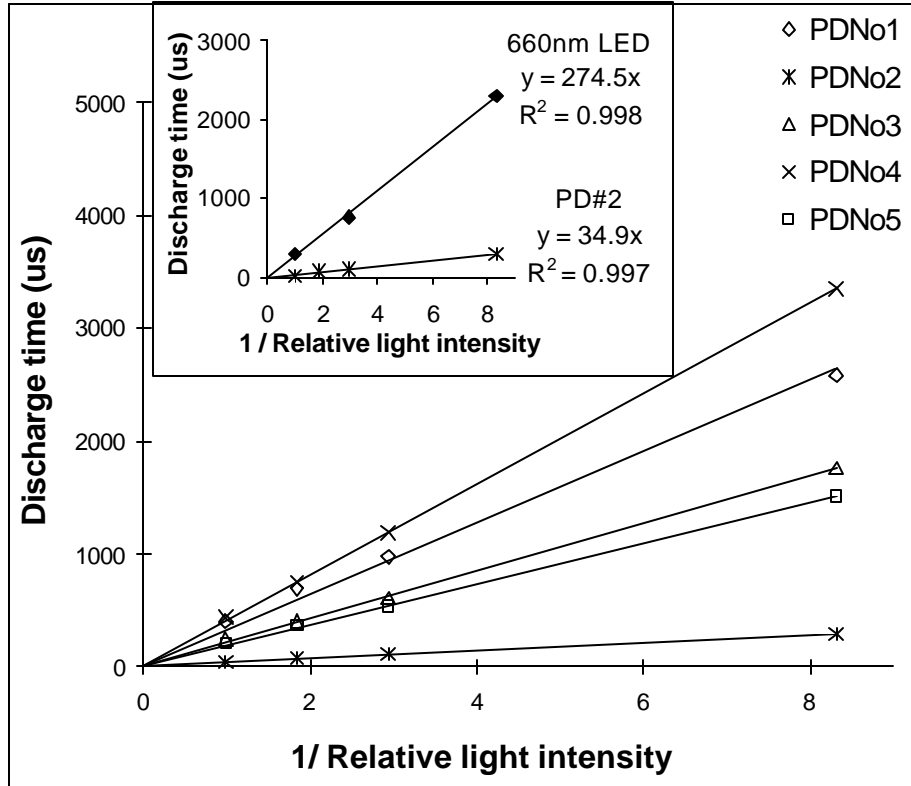


Figure 7

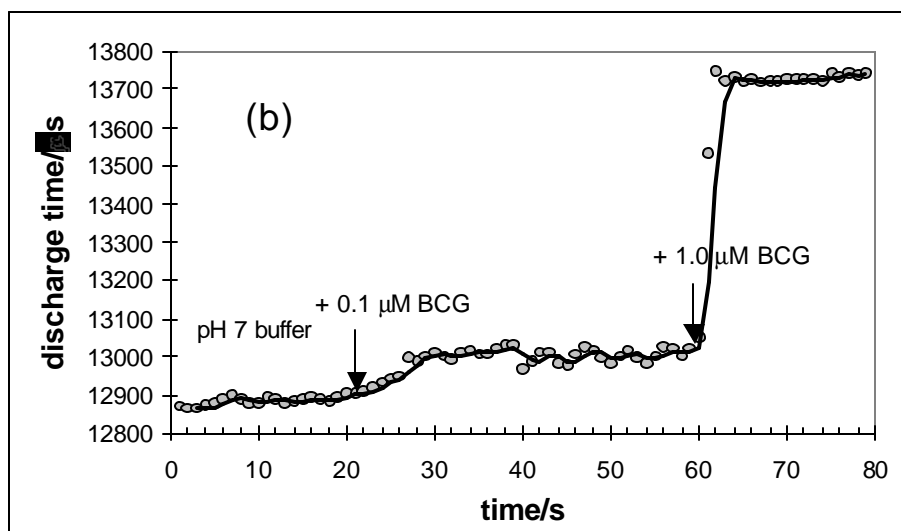
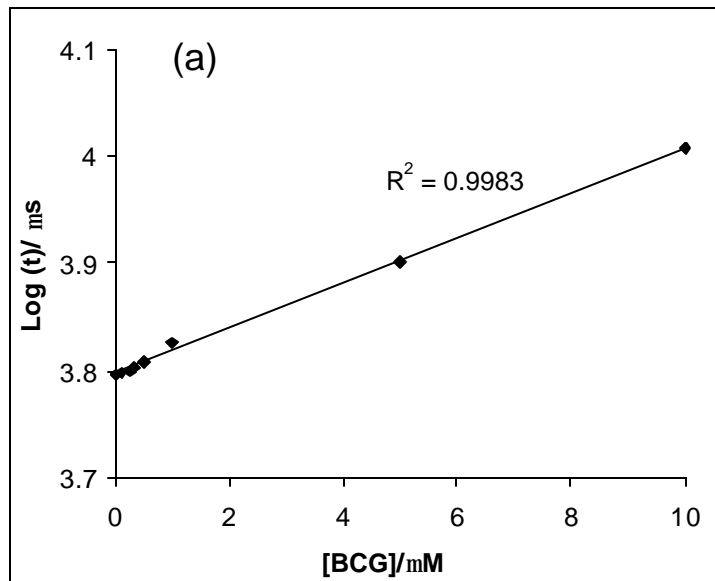


Figure 8

